Optimization of Multicomponent Photopolymer Formulations Using High-Throughput Analysis and Kinetic Modeling

Peter M. Johnson and Christopher N. Bowman
University of Colorado at Boulder, Dept. of Chemical and Biological Engineering, Boulder, CO 80309

Jeffrey W. Stansbury
University of Colorado at Boulder, Dept. of Chemical and Biological Engineering, Boulder, CO 80309, and University of Colorado Denver, Dept. of Craniofacial Biology, Aurora, CO 80045

DOI 10.1002/aic.12055
Published online September 8, 2009 in Wiley InterScience (www.interscience.wiley.com).

While high throughput and combinatorial techniques have played an instrumental role in materials development and implementation, numerous problems in materials science and engineering are too complex and necessitate a prohibitive number of experiments, even when considering high throughput and combinatorial approaches, for a comprehensive approach to materials design. Here, we propose a unique combination of high throughput experiments focused on binary formulations that, in combination with advanced modeling, has the potential to facilitate true materials design and optimization in ternary and more complex systems for which experiments are never required. Extensive research on the development of photopolymerizable monomer formulations has produced a vast array of potential monomer/comonomer, initiator and additive combinations. This array dramatically expands the range of material properties that are achievable; however, the vast number of potential formulations has eliminated any possibility of comprehensive materials design or optimization. This limitation is addressed by maximizing the benefits and unique capabilities of high throughput experimentation coupled with predictive models for material behavior and properties. The high throughput experimentation-model combination is useful to collect a limited amount of data from as few as 11 experiments on binary combinations of 10 analyzed monomers, and then use this limited data set to predict and optimize formulation properties in ternary resins that would have necessitated at least 1000 high throughput experiments and several orders of magnitude greater numbers of traditional experiments. A data analysis approach is demonstrated, and the model development and implementation for one model application in which a range of material properties are prescribed, and an optimal formulation that meets those properties is predicted and evaluated. © 2009 American Institute of Chemical Engineers *AIChE J,* 56: 1262–1269, 2010
Keywords: photopolymerization kinetics, modeling, parameter optimization

Introduction

Photopolymerization is ubiquitously implemented for a range of biological, high technology and conventional applications including photolithography, coatings, dental

Additional Supporting information may be found in the online version of this article.

Correspondence concerning this article should be addressed to C. N. Bowman at Christopher.bowman@colorado.edu

materials, contact lenses, tissue engineering and adhesives due to their wide range of formulations and rapid, solvent-free processing.[1–3] The material requirements for these applications generally involve a multicomponent formulation containing a variety of reactive species, initiators, and other components such as fillers, pigments and dyes to achieve the desired reaction kinetics and material properties. This complexity hinders the optimization of formulations due to the large available parameter space, and is further complicated by the nonlinear responses in photopolymerization kinetics and related material properties as formulation changes are made. As monomer conversion proceeds, radical diffusion rates are inhibited whereas monomer diffusion remains rapid, causing a nontypical increase in the polymerization rate, or autoacceleration. When the polymerization reaches an even higher double bond conversion, the monomer mobility is also restricted, and this restriction leads to a rapid decrease in polymerization as a function of conversion, or autodeceleration. While autoacceleration generates higher initial polymerization rates; autodeceleration leads to unreacted double bonds remaining in the polymer.[4,5] These phenomena are complicated significantly by the fact that the diffusion coefficients of monomer and polymer are changing by as many as 6–10-orders of magnitude in a polymerizing system that may react in as little as 1–10 s.

These complexities have led to the development of models for photopolymerization kinetics, which are mainly limited to single monomer systems due to computational restraints and were only recently developed and tested for multicomponent formulations.[6–9] To alleviate the experimental bottleneck, a procedure was developed to allow for a high-throughput analysis of photopolymer conversion. This method uses gradients of exposure time and composition to determine the conversion of a binary formulation on a single sample, greatly increasing the throughput of photopolymer kinetic analysis.[10–13] Results from this work have shown a need to balance both the crosslinking monomers and the monovinylic monomers to achieve optimal kinetics and polymeric material properties. Simplistically, high crosslinking densities lead to the formation of a heterogeneous network that contains residual unsaturation and has increased brittleness, whereas high levels of monovinylic monomers reduce the photopolymerization rate and lower the modulus and glass transition temperature of the fully polymerized material. However, even with high-throughput analysis techniques, limitations remain in the parameter space that can be analyzed in a reasonable time. If, as nearly all do, a photopolymer formulation contains more than two components, high-throughput analysis methods require a prohibitive amount of time to implement over the complete range of available formulations.

In response to the limitations of even high-throughput analytical techniques, kinetic parameters optimized from high-throughput analysis data of binary systems were extended through a kinetic model to predict photopolymerization kinetics for multicomponent formulations. This work integrates this multicomponent photopolymerization model with fundamental models of material properties to predict both photopolymerization kinetics and material properties. A model optimization protocol estimates kinetic parameters to predict material properties of a wide range of formulations while using only a limited experimental data set collected through high-throughput analysis techniques. This analysis is then utilized to perform materials design and optimization for a model application.

Experimental

Materials

Dipropylene glycol diacryate (DPGDA) and triethylene glycol diacryate (TEGDA) were obtained from Sartomer (Exton, PA). Ethoxylated (1 EO/Phenol) bisphenol A diacrylate (EBADA), tetrahydrofurfuryl acrylate, ethyl hexyl acrylate, and dodecyl acrylate (DDA) were obtained from Aldrich Chemicals (Milwaukee, WI) and used as received. Hexyl acrylate (HA) and hexanediol diacrylate (HDDA) were obtained from Fisher Chemicals and used as received. Benzyl carbamate acrylate (BCA) was synthesized using a procedure detailed elsewhere.[14] Bisphenol A glycidyl acrylate (BisGA) was provided by Cytec, Inc. The photoinitiator 2,2-dimethoxyacetophenone (DMPA) was obtained by Ciba-Giegy (Hawthorne, NY).

Thirteen compositions were formulated and tested to compare the model to the FTIR data for Figure 4. All formulations had 0.5 wt % DMPA, and the monomer composition follows for the 13 samples: 5/30/65 wt % THFFA/EHA/EBADA (1), 40/35/25 wt % HDDA/HA/EHA (2), 10/35/55 wt % HA/DDA/TEGDA (3), 40/45/15 wt % THFFA/BisGA/EBADA (4), 5/50/45 wt % HDDA/THFFA/DPGDA (5), 30/60/10 wt % HA/THFFA/DDA (6), 25/10/65 wt % HA/TEGDA/EBADA (7), 10/55/35 wt % HDDA/EHA/DDA (8), 25/10/65 wt % HA/THFFA/BisGA (9), 70/25/5 wt % HDDA/DPGDA/EBADA (10), 55/10/35 wt % HA/EHA/DPGDA (11), 35/35/30 wt % BisGA/EHA/EBADA (12), and 20/20/60 wt % THFFA/EHA/TEGDA (13).

High-throughput analysis of photopolymer conversion

Fourier transform infrared (FTIR) studies were conducted with a modified FTIR microscope (Nicolet Continuμm, Thermo-Nicolet, Madison, WI) after exposure time and composition gradients have been generated on the sample. This process has been described in detail elsewhere.[7,8,11,12] Reaction details and sample preparation are detailed in the Supplemental Information. The modifications allow for faster analysis of conversion using a continuous collection of spectra as the motion stage moves across the sample in a predefined path. This high-throughput technique produces a data set of 1250 spectra in an array of 10 compositions and 125 exposure times in 24 min.

Photopolymerization kinetic modeling

A model for photopolymerization kinetics was created using free volume polymerization kinetics with previous publications detailing the underlying kinetics and reactions included in the model.[7,8,15–17] A brief description of the parameters that dictate photopolymer kinetics in the model is given here. The free volume of the formulation is used to assess the impact of the conversion change on mass transfer, which is subsequently utilized to determine propagation and termination kinetic constants for each monomer type as a

function of the composition and reaction extent. The propagation and termination kinetic constants used in this work include Arrhenius temperature dependence and resistances dependent on free volume and reaction-diffusion kinetics. These kinetic parameters are given in Eqs. 1 and 2, and contain the kinetic parameters that are optimized for each monomer

$$k_p = k_{p0}\,\exp(-E_{Ap}/R_{gas}T)(1+\exp(A_p(1/f-1/f_{cp})))^{-1} \quad (1)$$

$$k_t = k_{t0}\exp(-E_{At}/R_{gas}T) \times\left(1+\frac{1}{Rk_p[M_{tot}]/(k_{t0}\exp(-E_{At}/RT))+\exp(A_t(1/f-1/f_{ct}))}\right)^{-1} \quad (2)$$

k_{p0} is the pre-exponential kinetic factor for the true reaction kinetic constant for the chemical reaction of radical propagation through unreacted carbon-carbon double bonds of the same monomer type. Similarly, k_{t0} is the pre-exponential kinetic constant for the bimolecular termination reaction of two radicals, f is the fractional free volume of the polymerizing solution, f_{cp} and f_{ct} are the critical fractional free volumes where propagation and termination transition to diffusion control. A_p and A_t govern the rate at which the propagation and termination kinetic parameters decrease as the polymerization becomes diffusion controlled. These six kinetic parameters are optimized for each monomer from the high-throughput data set. E_{Ap} and E_{At} are the Arrhenius based activation energies for propagation and termination, respectively, and R is the reaction diffusion parameter. M_{tot} is the concentration of unreacted double bonds, and R_{gas} is the gas constant. Kinetic parameters for reactions containing a radical and monomer of different types are calculated using reactivity ratios.[18]

The model predicts the double bond concentration and reaction rate for each monomer species, radicals, oxygen, and initiators as a function of time. From this information, the photopolymer conversion is determined at each time point. In addition, the post exposure polymerization, commonly called dark polymerization, is also calculated. This additional assessment is required to capture the polymerization that occurs from radicals that remain after the light is extinguished. This equation assumes constant lumped k_p and k_t over the entirety of the dark polymerization and is shown in Eq. 3

$$M_{tot} - M_{tot,0} = \frac{k_{pL}M_{tot}}{2k_{tL}}\ln(2k_{tL}R_0t+1) \quad (3)$$

R_0 is the sum of both radical concentrations when the light is turned off, while k_{pL} and k_{tL} are the lumped kinetic parameters. These lumped parameters are averaged using the volume fractions of the monomer concentration at the point that the light is extinguished. $M_{tot,0}$ is the double bond concentration at the point the light exposure ceases. Dark polymerization is significant during autoacceleration and is required to obtain an accurate profile.

The optimization protocol uses a particle swarm optimization to estimate kinetic parameters from high-throughput conversion data. Previous publications have determined kinetic parameters for multiple monomers, producing statistically similar kinetic parameters in each case.[7] Once kinetic parameters are optimized, conversion for all possible formulations is readily modeled. A tertiary diagram is modeled in 5 wt % increments for every possible ternary and lower order formulation.

High-Throughput Analysis for Kinetic Modeling of Photopolymers

The modeling of benzyl carbamate acrylate (BCA) and its inclusion in the materials design process is demonstrated here to show the technique by which additional monomers are incorporated in the multicomponent formulation model. BCA was chosen as a monomer to integrate into the system because prior work has shown significantly enhanced photopolymerization kinetics when it is added as a reactive diluent.[19] BCA polymerizes to nearly 100% conversion in a short period of time and is readily miscible with both hexyl acrylate (HA) and hexanediol diacrylate (HDDA). For the modeled results, the kinetic parameters of hexyl acrylate and hexanediol diacrylate were unchanged from prior optimization protocols.[7]

Hexyl acrylate and benzyl carbamate acrylate results and model predictions

The copolymerization of BCA and HA was analyzed using the high-throughput conversion to generate a conversion data set to optimize the kinetic parameters for BCA. The high-throughput conversion data and modeled results are shown in Figure 1a and 1b, respectively. This plot demonstrates the highly nonlinear nature of the dependence of the polymerization kinetics and conversion on both composition and exposure time that must be accounted for in the model. In Figure 1a, the fastest photopolymerization rates occur in compositions greater than 80 wt % BCA. While pure BCA polymerizes slightly more rapidly than 80 wt % BCA, photopolymerization in this region is rapid due to both the kinetics and extensive dark polymerization. After 30 s of exposure, compositions with less than 30 wt % HA reach conversions above 98%. Additional amounts of hexyl acrylate reduce the photopolymerization kinetics, with the reduction greater than expected simply by averaging the individual kinetic rates.

The photopolymerization model does not predict the system response accurately unless the reactivity ratios vary from unity for this copolymerization. This deviation from equal reactivity ratios is due to intermolecular interactions and has been confirmed from other studies of novel acrylates.[14,20] From the model optimization, the propagation kinetic constant k_{p0}, was found to be higher than any other monomer, and the optimized reactivity ratios result in the preferential incorporation of BCA into the polymer chain. These kinetic parameters result in a slightly higher conversion for BCA as compared to HA at any given exposure time. Kinetic parameters for BCA were only optimized using the data provided in Figure 1a.

Although no experimental copolymerizations of BCA and HDDA, even as a binary system, were performed, polymerizations throughout the entire ternary composition space of BCA, HA, and HDDA were modeled successfully using

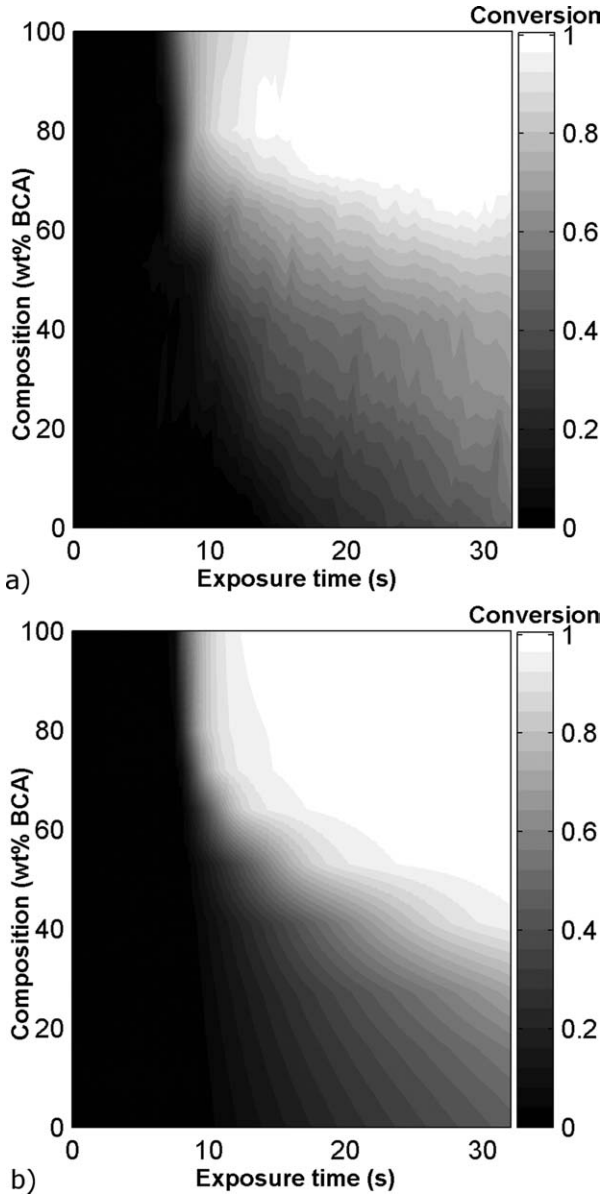

Figure 1. Conversion grayscale map for HA-BCA formulations using high-throughput analysis (a), and the resulting optimized model (b).

Polymerization conditions were a light intensity of 3.5 mW/cm^2 with 0.5 wt % DMPA at 23 °C. Modeling was performed at the same conditions, with time and composition points matching all points of the high-throughput data plot.

kinetic parameters for HA and HDDA from previous studies, and BCA from the data shown in Figure 1.[8] A large region of the potential formulation space indicates that the overall acrylate conversion reaches nearly 100% at 30 s of exposure time. This modeled ternary composition plot for 30 s exposure time is shown in Figure 2. Because this region of high conversion is large, a single gradient was tested within the region using all three monomers to produce a composition gradient with similar kinetics regardless of composition. A gradient from 80/20 wt % BCA/HA to 65/35 wt % HDDA/HA was tested, with the gradient along the line illustrated in Figure 2, with results and the model prediction shown in Figure 3a and 3b. Results in Figure 3 are reported as a percentage of each formulation, not as discrete monomers.

From Figure 3, all systems reach a minimum of 97% conversion at 30 s, regardless of composition. At 18 s of exposure time, conversion for all systems is greater than 94%. Higher amounts of BCA increase both the polymerization rate and reduce the oxygen inhibition time. This result is due to the increased propagation rate for novel monomers and the reduction of inhibitor as compared to the HA/HDDA formulation. The model shows a more rapid photopolymerization than seen in the experimental results, but shows similar trends as compared to the experimental results, with an increasing amount of BCA showing a faster polymerization rate and a shorter exposure time to full conversion. In addition, 13 ternary formulations were selected from the available monomer set and polymerized under the same conditions as the model. Figure 4 details the conversion for 13 ternary formulations after 30 s exposure, with the details of all formulations listed in the Materials section. The predicted conversion from the model is in excellent agreement with the experimental conversion, being within the 95% confidence interval of the experimental conversion value for nine of the 13 compositions evaluated. The conversion error of the model is randomly distributed over the 13 formulations, with an average error of 3.7%. Only two compositions have a model prediction error larger than 6% and accurately predict the correct formulation conversion in systems with high crosslink density.

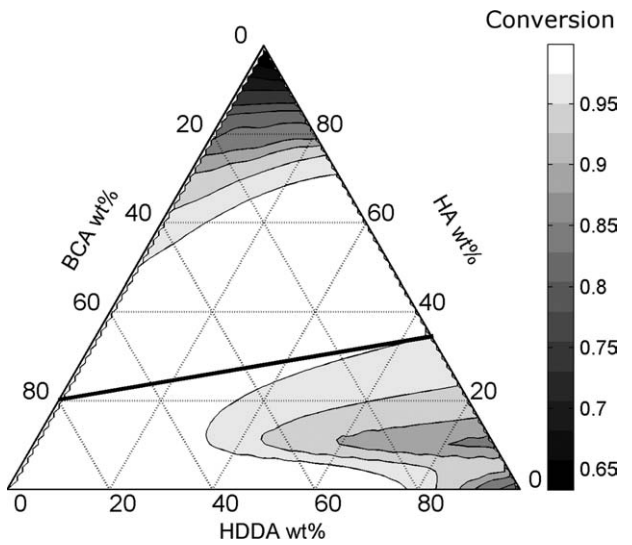

Figure 2. Modeled conversion at 30 s for the BCA/HA/HDDA ternary formulation space, using only optimized kinetic parameters.

Model conditions were at a light intensity of 3.5 mW/cm^2 with 0.5 wt % DMPA at 23 °C, including oxygen inhibition. The black line denotes the gradient analyzed experimentally in Figure 3, and denotes a line of nearly complete conversion regardless of composition.

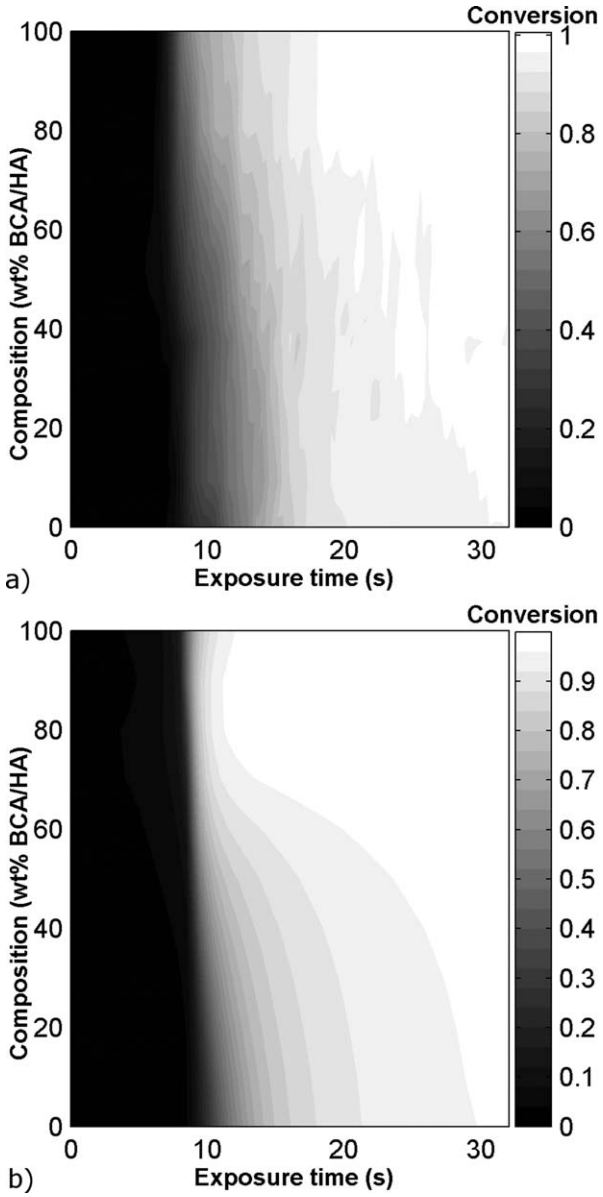

Figure 3. Conversion grayscale map for the high-throughput analysis (a), and the optimized predictive model (b), using a composition gradient from 80/20 wt % BCA/HA to 65/35 wt % HDDA/HA.

Polymerization conditions were a light intensity of 3.5 mW/cm^2 with 0.5 wt % DMPA at 23 °C. Modeling was performed at the same conditions, with time and composition points matching all points of the high-throughput data plot.

Material Design for Photopolymer Formulations

Photopolymer property modeling

When considering materials design, if the possible formulations are limited to ternary systems with monomer compositions varying by steps of 5%, 10 possible monomers would require the evaluation of 21385 discrete formulations. By utilizing high-throughput sampling, that number is reduced to *only* 1069 high-throughput samples that would need to be analyzed. Quaternary and higher component formulations would require exponentially more measurements. Instead, by combining high throughput experiments on 11 different binary monomer compositions with modeling of the polymerization kinetics and material properties, predictions are accessible for the entire composition range, enabling one to perform true optimization of the photopolymerizable composition. Here, for simplicity of presentation, only ternary and simpler systems are considered; however, without any additional experiments the approach is appropriate for considering formulations of as many components as desired.

All formulations are modeled for exposure times ranging from 0 to 40 s, with conversion calculated at each time point. The same initiation conditions were used as given for the high-throughput data. Dark polymerization is included for every exposure time, and exposure times were limited to a maximum of 40 s. Once the acrylate conversion and composition are known for a proposed composition, critical material properties to be used as design criteria are predicted such as modulus, density and glass transition temperature. The fraction of monomer extractable (f_{ex}), crosslink density (v_d), and resulting rubbery modulus (E) are calculated using the following equations[21]

$$f_{ex} = \sum_i (1 - X_i)^{fi} w_i \tag{4}$$

$$v_d = \sum_{DA} X_i^2 [C = C]_i / 2 \tag{5}$$

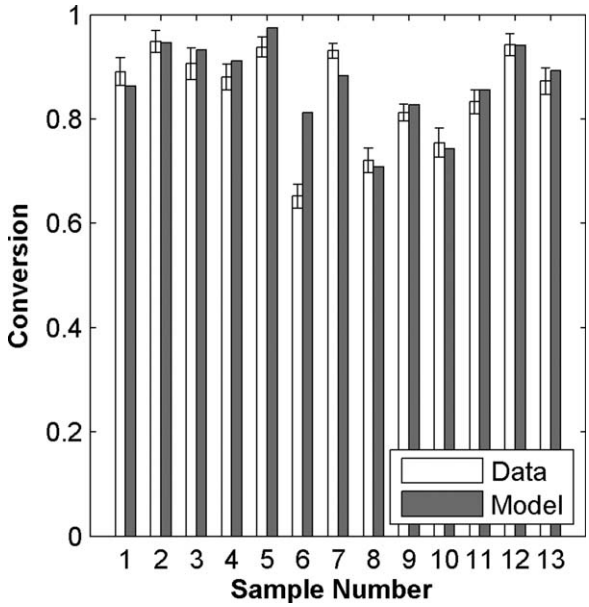

Figure 4. Conversion at 30 s exposure time for 13 randomly chosen ternary formulations as measured by FTIR and predicted by the model.

The average deviation between the model and experiment is 3.7% conversion. Sample compositions are defined in the Materials section.

Table 1. Polymer Property Limitations for a High Glass Transition Temperature, Low Monomer Extractable Formulation

Material Property	Limitations
Rubbery modulus	$E > 5.0$ MPa
Glass transition temperature	$T_G > 323$ K (50 °C)
Fraction of monomer extractable	$f_{ex} < 5\%$
Viscosity	η: 5-45 mPa·s
Shrinkage	$v_s < 10$ %

$$E = 3v_d RT \tag{6}$$

X_i, f_i, w_i, and $[C = C]_i$ are the conversion, number of double bonds, weight percent, and double bond concentration of monomer i. Eq. 4 is presented for diacrylate monomers although it is obviously readily extendable to all compositions and acrylate types. In Eq. 6, R is the gas constant, and T is the absolute temperature.

Using weighted averaging and predictive models, further material properties are readily calculated. Glass transition temperature (T_G), viscosity (η), and percent shrinkage (p_s) are calculated as follows[22,23]

$$T_G = \frac{(\alpha_m T_{Gm} + (\alpha_p T_{Gp} v_p - \alpha_m T_{gm})X)}{(\alpha_m v_m + (\alpha_m v_m - \alpha_m v_m)X)} \tag{7}$$

$$\ln \eta = \sum_i w_i \ln \eta_i \tag{8}$$

$$p_s = \sum_i v_S [C = C]_{i0} X_i / 100 \tag{9}$$

In Eq. 7, the parameters T_{Gm}, T_{Gp}, α_m, α_p, v_m and v_p represent the monomer and polymer glass transition temperatures, coefficients of thermal expansion and specific volume, respectively. Viscosity of each monomer, η_i, is logarithmically averaged to produce a formulation viscosity. For percent shrinkage, v_S is the volume shrinkage after a double bond is polymerized, and described and validated in detail elsewhere.[24] All of these polymer properties are predicted at every composition, exposure time and conversion.

These material property formulas were used with the conversion-composition data set to produce estimated material properties for every possible composition. To screen such a large data set, limitations to any predicted material property are compared against the data set to determine if the specified formulation and exposure time result in a prediction that meets the constraint. By limiting the desired value of any single polymer property, such as the percent of monomer extractable or the glass transition temperature, for example, a large composition range is immediately excluded from the potential monomer composition-exposure time space. Limitations are screened sequentially, and the possible formulations are reduced as those that do not meet these constraints are removed.

In considering the design of a scratch resistant, high-glass transition temperature coating as a model material to demonstrate the optimization process, it would generally be desired to produce a crosslinked polymer with a minimum glass transition temperature, a minimum rubbery modulus (or crosslink density), and no more than a certain amount of residual monomer that was extractable (i.e., unreacted). In addition, a maximum shrinkage level and an appropriate range of viscosities would be desired, all within the context of meeting those specifications at a minimum cost. As an example design specification, parameter limitations such as these are given in Table 1. Clearly, without an impractical number of high throughput experiments, it would not be possible to perform this constrained optimization. Here, the combination of a minimum number of experiments and the model enables the optimization to be completed.

Each of these polymer property constraints in turn constrains the available formulations and exposure times. Certain parameters have a far more significant effect than others, with the glass transition temperature constraint ($T_G >$ 323 K) causing 53% of the potential formulations to be excluded. In comparison, this particular viscosity constraint removes only 36% of the potential formulations, because eight of the 10 monomers in these data set have viscosities lower than the constraint of 45 mPa·s. When these two constraints are combined, 83% of the potential formulations are removed from the data set, showing the two constraints had minimal overlap. When all five constraints are applied, a significant ternary composition-exposure time space remains, all of which meet the entire list of specified properties. It is worth noting, however, that despite the wide range of compositions for which these properties can all be satisfied, there is no purely binary composition that achieves all of the desired properties. Thus, none of the compositions experimentally characterized would, by themselves be able to achieve all the desired properties. In Figure 5, the various properties are plotted for one range of ternary compositions that meets all of the desired properties. Predicted conversions and estimated polymer properties for the BCA/DDA/TEGDA formulation space are given in the Supplemental Information.

These ternary plots allow for easy visual analysis of changes caused by variations in monomer content. The reduction in the TEGDA content increases the overall conversion due to the reduction in the crosslink density, leading to a lower percent extractables and higher glass transition temperature. Additional dodecyl acrylate (DDA), an alkyl monoacrylate, reduces the overall glass transition temperature as it has the lowest pure glass transition temperature of the three monomers in the ternary formulation. In this ternary formulation, only 6% of the overall ternary formulation space remains, and this process has reduced a complex formulation search into a more manageable area for detailed analysis. Further analysis is performed here based on optimization of the cost function, which takes into account the formulation cost and the processing cost associated with the reaction time needed for a given formulation. In this case, the formulation and processing costs were estimated, with monomer prices increasing from DDA as the lowest to BCA as the highest, based on both commodity pricing and specialty chemical pricing for those monomers for which commodity prices are not available. Irradiation cost was based on a fixed cost per unit exposure time. Information on costs is included in the Supplemental section for a more thorough

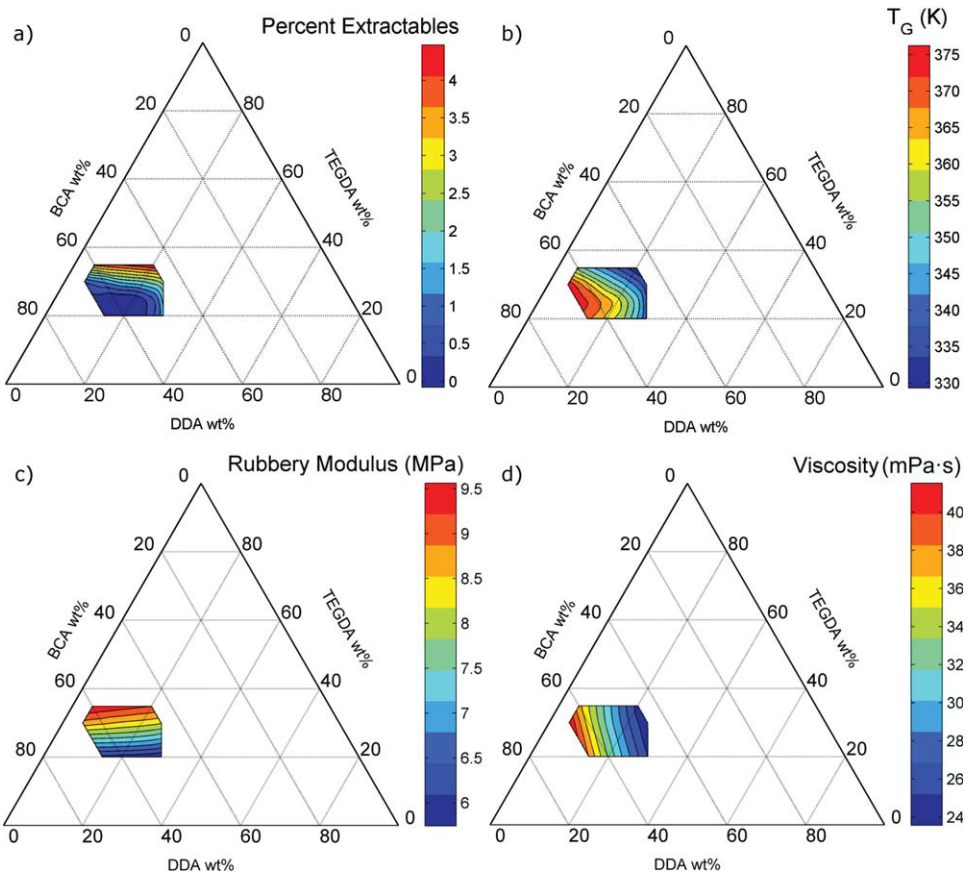

Figure 5. BCA/DDA/TEGDA ternary diagrams showing predicted percent extractables (a), glass transition (b), rubbery modulus (c), and viscosity (d) only in regions where all material parameters are met.

The limited composition range requires between 20 to 35 wt % TEGDA, 5 wt % to 30 wt % DDA, and 45 to 65 wt % BCA. The 20 wt % TEGDA boundary is due to the rubbery modulus limitation, which requires a certain level of crosslinking only possible with the diacrylate.

discussion. Figure 6 presents two different cases for the cost function of this system, one where processing costs are on the order of a typical application, therefore, valuing exposure time, and another where the processing costs are reduced by 10 times such that monomer cost dominates the optimal formulation determination.

When compared with the material properties in Figure 5, the highest cost region in both cases has the best application

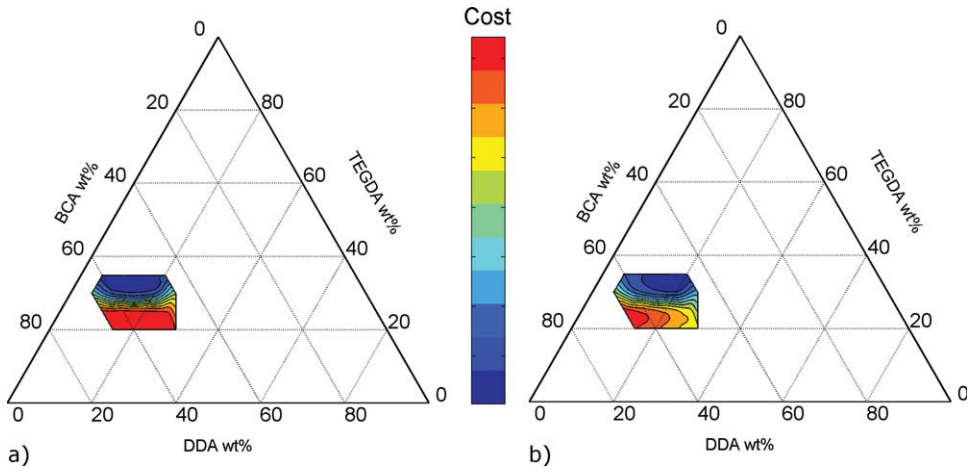

Figure 6. Cost estimates for the optimized BCA/DDA/TEGDA region using typical processing and monomer costs (a) and a system with processing costs reduced by a factor of 10 (b).

Cost values are normalized in each diagram to the minimum value. Decreased processing costs causes monomer costs to influence the diagram, where the additional monomer cost of BCA as compared to the reduction of exposure time increases costs.

performance, with both the highest glass transition temperature and the lower percent extractables. In addition, a higher relative monomer cost introduces an increased cost due to BCA, which due to being a noncommercial monomer is assigned the highest cost. However, in both cases the addition of more TEGDA, the diacrylate, greatly reduces the cost function. This behavior is largely due to the reduced exposure time required with increasing TEGDA levels. Formulations containing 35 wt % TEGDA reach the specified parameters in 20–30% less exposure time than 20 wt % TEGDA formulations. This reduction in exposure time is far more significant in reducing the overall cost, even with reduced processing costs. This additional cost parameter allows for a better understanding of the optimization tradeoffs required for the application, and opens a pathway to determine regions of equivalent material property performance at equivalent or lower cost.

Conclusions

This design approach to photopolymerizable formulations provides a process to model and predict photopolymerization kinetics, and leverage this information to determine relevant materials properties. Ultimately, the advantage of the synergistic combination of a minimum number of experiments coupled to accurate kinetic and material property models enables an exciting development in the area of combinatorial and high throughput studies — that of true materials design and optimization. Here, we have demonstrated the value of this technique by analyzing a ternary composition and exposure parameter space that could not be evaluated experimentally. The result was an optimized cost formulation that met all the specific material properties of the model application.

Literature Cited

1. Decker C. The use of UV irradiation in polymerization. *Polymer Int.* 1998;45:133–141.
2. Decker C. New developments in UV radiation curing of protective coatings. *Surf Coat Int Part B-Coat Trans.* 2005;88:9–17.
3. Decker C. Recent developments in photoinitiated radical polymerization. *Macromol Symposia.* 1999;143:45–63.
4. Cramer NB, Reddy SK, O'Brien AK, Bowman CN. Thiol-ene photopolymerization mechanism and rate limiting step changes for various vinyl functional group chemistries. *Macromol.* 2003;36: 7964–7969.
5. Reddy SK, Anseth KS, Bowman CN. Modeling of network degradation in mixed step-chain growth polymerizations. *Polymer.* 2005; 46:4212–4222.
6. Lovestead TM, O'Brien AK, Bowman CN. Models of multivinyl free radical photopolymerization kinetics. *J Photochem Photobio A-Chem.* 2003;159:135–143.
7. Johnson PM, Stanbury JW, Bowman CN. Alkyl chain length effects on copolymerization kinetics of a monoacrylate with hexanediol diacrylate. *J Comb Chem.* 2007;9:1149–1156.
8. Johnson PM, Stansbury JW, Bowman CN. Kinetic modeling of a comonomer photopolymerization system using high-throughput conversion data. *Macromol.* 2008;41:230–237.
9. Andrzejewska E, Bogacki MB, Andrzejewski M, Tyminska B. Modeling of the kinetics of polymerization of dimethacrylates. The kinetic constants vs. termination mechanism. *Polimery.* 2000;45: 502–513.
10. Johnson PM, Stansbury JW, Bowman CN. Photopolymer kinetics using light intensity gradients in high-throughput conversion analysis. *Polymer.* 2007;48:6319–6324.
11. Johnson PM, Stansbury JW, Bowman CN. High-throughput kinetic analysis of acrylate and thiol-ene photopolymerization using temperature and exposure time gradients. *J Polym Sci, Part A: Polym Chem.* 2008;46:1502–1509.
12. Johnson PM, Reynolds TB, Stansbury JW, Bowman CN. High throughput kinetic analysis of photopolymer conversion using composition and exposure time gradients. *Polymer.* 2005;46:3300–3306.
13. Lovell LG, Stansbury JW, Syrpes DC, Bowman CN. Effects of composition and reactivity on the reaction kinetics of dimethacrylate dimethacrylate copolymerizations. *Macromol.* 1999;32:3913–3921.
14. Kilambi H, Reddy SK, Schneidewind L, Stansbury JW, Bowman CN. Copolymerization and dark polymerization studies for photopolymerization of novel acrylic monomers. *Polymer.* 2007;48:2014–2021.
15. Goodner MD, Bowman CN. Modeling primary radical termination and its effects on autoacceleration in photopolymerization kinetics. *Macromol.* 1999;32:6552–6559.
16. Goodner MD, Lee HR, Bowman CN. Method for determining the kinetic parameters in diffusion-controlled free-radical homopolymerizations. *Ind Eng Chem Res.* 1997;36:1247–1252.
17. Bowman CN, Kloxin CJ. Toward an enhanced understanding and implementation of photopolymerization reactions. *AIChE J.* 2008; 54:2775–2795.
18. Buback M, Muller E. Propagation kinetics of binary acrylate-methacrylate free-radical bulk copolymerizations. *Macromol Chem Phys.* 2007;208:581–593.
19. Kilambi H, Beckel ER, Berchtold KA, Stansbury JW, Bowman CN. Influence of molecular dipole on monoacrylate monomer reactivity. *Polymer.* 2005;46:4735–4742.
20. Kilambi H, Stansbury JW, Bowman CN. Deconvoluting the Impact of intermolecular and intramolecular interactions on the polymerization kinetics of ultrarapid mono(meth)acrylates. *Macromol.* 2007;40: 47–54.
21. Flory PJ. *Principles of Polymer Chemistry*. Ithaca, NY: Cornell University Press; 1953.
22. Stansbury JW, Trujillo-Lemon M, Lu H, Ding XZ, Lin Y, Ge JH. Conversion-dependent shrinkage stress and strain in dental resins and composites. *Dental Mater.* 2005;21:56–67.
23. Kannurpatti AR, Anseth JW, Bowman CN. A study of the evolution of mechanical properties and structural heterogeneity of polymer networks formed by photopolymerizations of multifunctional (meth)acrylates. *Polymer.* 1998;39:2507–2513.
24. Lu H, Stansbury JW, Bowman CN. Impact of curing protocol on conversion and shrinkage stress. *J Dental Res.* 2005;84:822–826.

Manuscript received May 4, 2009, and revision received Aug. 2, 2009.